Central European Journal of Energetic Materials
ISSN 1733-7178; e-ISSN 2353-1843

Cent. Eur. J. Energ. Mater. 2022, *19*(2): 113-134; DOI 10.22211/cejem/150827
Article is available in PDF-format, in colour, at:
https://ipo.lukasiewicz.gov.pl/wydawnictwa/cejem-woluminy/vol-19-nr-2/

Research paper

Experimental Study of the Effectiveness of a Model Reactive Armour without Metal Plates

Waldemar A. Trzciński*), Karol Zalewski, Zbigniew Chyłek, Leszek Szymańczyk

Military University of Technology, 2 gen. S. Kaliskiego Street, 00-908 Warsaw 46, Poland
* *E-mail:* waldemar.trzcinski@wat.edu.pl

ORCID information:
Trzciński W.A.: https://orcid.org/0000-0002-8313-6434
Zalewski K.: https://orcid.org/0000-0002-4563-8767
Chyłek Z.: https://orcid.org/0000-0003-1799-4534
Szymańczyk L.: https://orcid.org/0000-0002-5071-8526

Abstract: Explosive reactive armour (ERA) is widely used to protect military vehicles against shaped charges and kinetic projectiles, but the use of the ERA element with metal plates is potentially hazardous to the surroundings. A patent claim has recently been issued on explosive reactive armour without metal plates. The non-metallic ERA consists of an explosive, a heavy metal powder and a binder. The aim of the present work was to experimentally test the effectiveness of such armour for disrupting cumulative jets. HMX was used as the explosive matrix and RTV silicone as the binder. Tungsten (W) powder was added to the explosive. The disruption of the cumulative jet was assessed on the basis of X-ray images, the number and size of holes in a steel plate, which was placed under the shaped charge, and the penetration depth of a steel target. It was shown that reactive armour consisting of HMX and W powder was effective in dispersing the cumulative jet, especially for a small impact angle (30°). The influence of the W particle size

and the content of the W powder in the armour on jet were investigated. Finally, the effectiveness of one of the tested reactive armours was compared with that of classic reactive armour with steel plates.

Keywords: reactive armour, metalized explosives, jet penetration

1 Introduction

Shaped-charge warheads and kinetic energy penetrators are known to pierce steel armour walls. However the penetrating effect of a shaped charge or kinetic energy penetrator can be effectively weakened by reactive armour elements. Usually, the reactive armour element is a multi-layer structure including plates made of metal or a composite material and at least one intermediate layer of an explosive or any other energetic material [1]. Upon initiation of the energetic material by the jet or rod, the released gases drive the plates and displace them away from thetarget. The heavy metal plates disrupt the metallic jet or damage and break up a kinetic energy penetrator, weakening their penetrating efficiency [2]. The reactive armour can also contain non-metallic plates such as ceramics, fiber reinforced plastics, aluminium and polyethylene [3, 4].

The explosive reactive armour (ERA) is the most effective protection against both shaped charges and kinetic projectiles, but the use of a fully detonable explosive in the element is hazardous to the surroundings due to metal fragments or moving plates. Another complication is that a conventional ERA is made of flat plates and is not suitable for protecting non-flat surfaces [5]. One proposal to reduce this threat while maintaining the effectiveness of the armour was to use non-detonating energetic materials instead of explosives [6, 7]. The authors of the patent [8] proposed a new reactive armour that reduces the lateral damage on the surroundings and can be easily applied to non-planar surfaces. The invention relates to a rigid or flexible reactive element for protection against shaped charges and kinetic projectiles. The element consists of a metallic or ceramic powder dispersed within a matrix of plastic explosive and a binder. 1,3,5,7-Tetranitro-1,3,5,7-tetrazoctane (HMX) and 1,3,5-trinitro-1,3,5-triazinane (RDX) can be used as the explosive component and hydroxyl-terminated polybutadiene (HTPB) or polydimethylsiloxane (PDMS) can be the binder. The metal powders proposed in the patent [8] are tungsten (W) powder with an average particle diameter of 120 mm, and tungsten carbide powder with an average particle diameter of 80 mm. The patent [8] does not specify the efficiency of the new reactive armour in dispersing the cumulated jet and its effectiveness in weakening jet

penetration into a steel target. The question we wanted to study is whether reactive armour composed of only explosive and W powder is effective in disrupting the cumulative jet.

The jet disturbance by an explosive layer with no other plates and an explosive layer with only one plate around it, was tested and numerically simulated in [9]. The experimental and numerical results were compared with those obtained for a two-plate ERA configuration. According to the authors of [9] it seems that the disruptive power of the flow of detonation products, although powerful, is limited and that a steel plate exhibits a much stronger disruptive power.

The aim of the present work was to experimentally test the effectiveness in disturbing a cumulative jet by a model reactive armour without steel plates, consisting of an explosive and W powder. HMX was the explosive matrix, and room temperature vulcanizable (RTV) silicone was used as the rubber. The jet dispersion was assessed by means of the pulse X-ray technique and by using a steel witness plate, and the jet penetration efficiency was tested in a steel target (rod). The influence of the W powder size, the powder content in the explosive composition, the reactive armour thickness and the angle between the jet direction and the armour surface, on the effectiveness of the reactive armour were investigated. A comparison of the effectiveness of one of the tested reactive armours and the classic armour with steel plates is also presented.

2 Materials

The metallized compositions were prepared using crystalline HMX (particle size below 75 μm) and two types of W powder. According to the technical data, the particle size of the first powder was between 5 and 50 μm (mean size 35 μm) and that of the second was between 1 and 10 μm (mean size 4.5 μm). Single-component condensation-type RTV silicone was used to bind the ingredients together.

The process of preparing the composition began with weighing out the appropriate amounts of HMX, W powder and RTV silicone. Initially, portions of silicone were added to the W powder. The mixture was continuously stirred. After a homogeneous mixture had been obtained, HMX was added with continuous stirring. Granules with the consistency of wet sand and of uniform colour were obtained and further elaboration was commenced. The resulting reactive mixture was transferred to an appropriate 3D printed mold. The entire charge was finally pressed using a hand press. The time from the addition of silicone to the completion of the elaboration process was only about 30 min,

due to the ongoing silicone cross-linking process. The prepared charges were left for 24 h. After this time the charges were relatively stiff and durable. The compositions of the formulations used in the tested reactive armours are presented in Table 1.

Table 1. Compositions of the formulations used in the tested reactive armours

Formulation	Particle size of W [μm]	Formulation composition [wt.%]			Average density [g/cm^3]
		HMX	W	Silicone	
PR-1	~35	28	60	12	3.46
PR-2	~4.5				3.23
PR-3		35	50	15	2.62
PR-4		42	40	18	2.22
PR-5		49	30	21	2.16

The reactive armour consisted of a formulation selected from Table 1, placed in the 3D printed mold made of PLA filament. The thickness of the mold wall was 1.5 mm. The reactive armour diameter was 120 mm, with variable thicknesses. The explosive layer was covered by a 1 mm thick filament plate.

3 Test Methods

Friction sensitivity measurements of the formulations obtained were made on a Julius Peters Apparatus according to the standard [10]. The impact sensitivity was determined by the Fall Hammer Method using a 5 kg drop hammer [11]. In both methods, the so-called lower sensitivity limit was determined, *i.e.* the minimum force (friction sensitivity) or the minimum impact energy of the hammer (impact sensitivity), for which at least one positive result was obtained in six consecutive trials.

In the set up for testing jet dispersion, the diagnostic shaped charge was placed above the reactive armour at a distance of 50 mm (Figure 1). The angle (α) between the armour surface and the axis of symmetry of the shaped charge was 90°, 60° or 30°. The medium caliber shaped charges were made of pressed PBXW-11 (85 g) and had sintered copper liners (24 g) with a cone shaped angle of 60° and a base diameter of 37 mm. The sintered liners were chosen for their availability. The charge casing and the lens were made of a 3D printing filament. The jet tip velocity, determined on the basis of images taken using X-ray photography at various times after the initiation of the shaped charge,

was 8300 m/s. The jets were linear and coherent, and the repeatability of the jet velocity was high (a deviation ±50 m/s).

In order to test the ability of the reactive armour to dissipate the cumulative jet, the technique of pulse X-ray (SCANDIFLASH) was used. In each test, X-rays were released after 35 μs from the moment of initiating the detonation of the shaped charge. In addition, a steel witness plate with a thickness of 2 mm and dimensions of 500×500 mm was placed at a distance of 500 mm under the armour. The plate was perpendicular to the symmetry axis of the shaped charge.

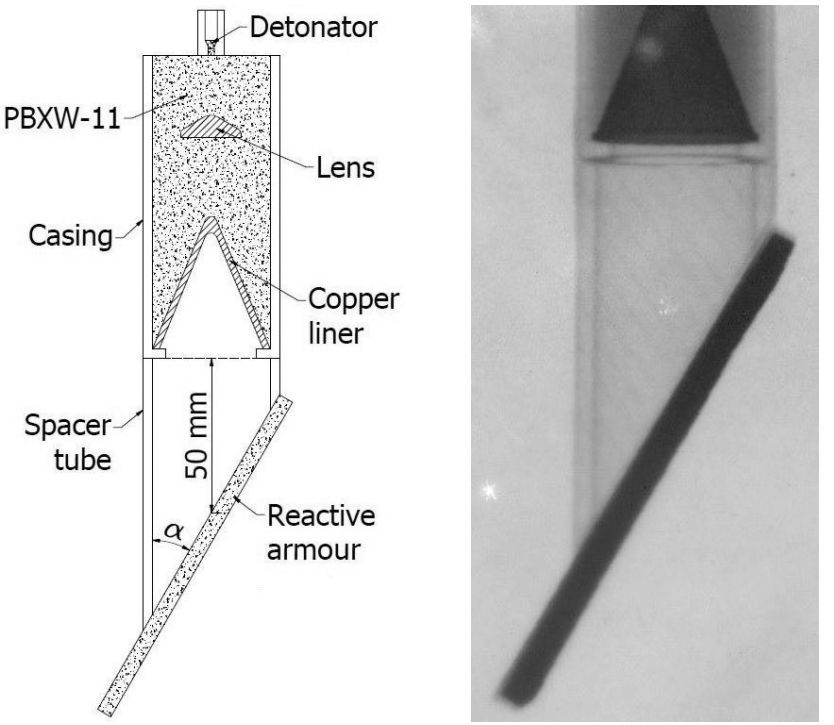

(a) (b)

Figure 1. Schematic and X-ray photo (inversion) of the set up for testing jet dispersion

To assess the effect of the reactive armour on the ability of the jet to penetrate a steel target, the system shown in Figure 2 was used. A mild steel rod with a diameter of 60 mm was used as the target. The tested reactive armour was placed between the shaped charge and the target. The standoff distance of the shaped charge was approximately 70 mm from the target surface for angles

α equal to 90° or 60° and about 90 mm for α = 30°. After the test, the steel rod was cut and the penetration depth was measured.

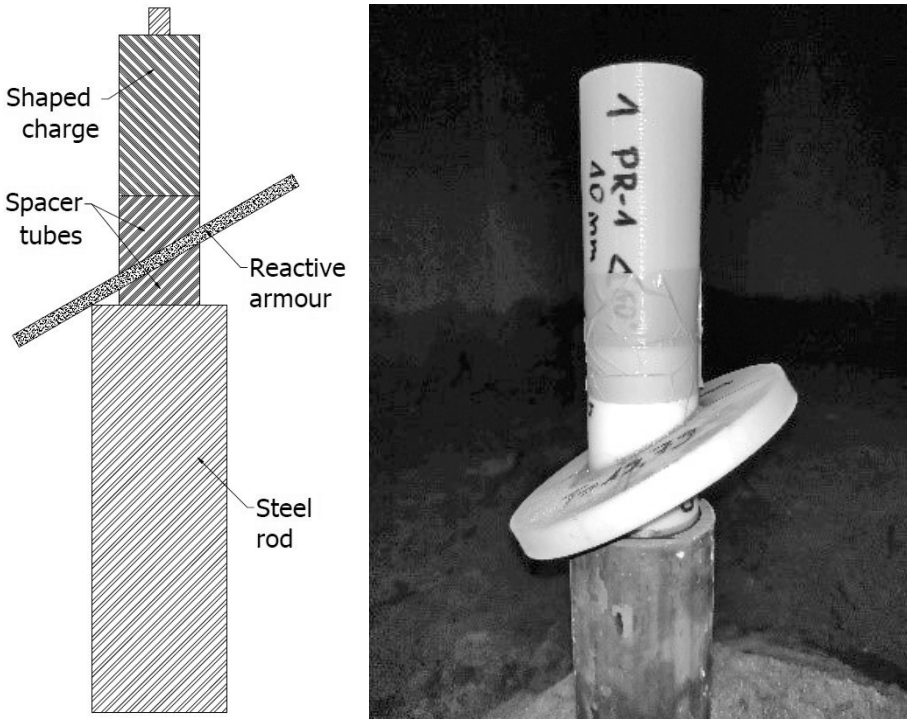

(a) (b)

Figure 2. Schematic and photo of the set up to test the jet penetration depth

4 Results and Discussion

From the tests performed on a Julius Peters Apparatus, it appears that the lower sensitivity limit was 172, 252 and 330 N for formulationsPR-1, PR-2 and PR-5, respectively. For comparison, the sensitivity of crystalline HMX was 149 N. The impact sensitivity determined by the Fall Hammer Method was 7.5 J for HMX, PR-1 and PR-2, and 10 J for PR-5. The tested mixtures are relatively sensitive to impact. Therefore, the process of elaborating the explosive composition with W particles should be improved in further research.

X-ray images of the cumulative jets taken at the same time (35 μs) after initiation of the shaped charge are shown in Figures 3-5 for different configurations

of the reactive armour. The photo in Figure 3(a) shows the undisturbed jet and a 100 mm long metal thin rod located 100 mm from the base of the copper liner. The rod was used to calibrate the photo.

The influence of the angle α on the degree of jet dispersion is shown in Figures 3(b-d) for the reactive armour PR-2 with a thickness of 10 mm. The reactive armour penetration by the jet at an angle of 90° generates a strong shock wave in the reactive material and HMX detonation is initiated. The detonation wave moves from the center of the charge (Figure 3(b)). The jet front is partially worn out by interaction with the W particles in the reactive material, but a tunnel free of these particles is probably formed in the armour at a later stage. W particles are accelerated in the direction of the detonation wave propagation. The photo shows that the front part of the jet is disturbed, but the rest of the jet is coherent. Lateral rarefaction waves in the explosion products and W particles behind the detonation wave do not disturb the jet. However, such an interaction is possible for angles less than 90°. In the case of setting the reactive armour at an angle of 60°, the jet is disturbed along its entire length, but it is still relatively continuous (Figure 3(c)). The jet is almost completely dispersed when the reactive armour angle is at 30° (Figure 3(d)). It should also be added that the penetration path of the jet into the reactive armour is extended to 11.5 mm for an angle of 60° and to 20 mm for an angle of 30°.

The effect of the reactive armour thickness on jet dispersion was investigated for the PR-1 armour (Figures 4(a) and 4(b)) and for the PR-2 armour (Figures 4(c), 4(d) and 3(d)). In all cases the jet impact angle was 30°. As would be expected, thicker explosive armour disrupts the jet more strongly. The analysis of the photos in Figures 4 and 3(d) shows that the reactive armour from the PR-2 formulation containing W particles with an average diameter of 4.5 μm are more effective in disturbing the jets than PR-1 armour containing larger W particles. It seems that the greater effectiveness of the reactive armour with finer W powder is due to the fact that this powder is more easily accelerated in the flow of detonation products in the rarefaction wave behind the detonation wave front and during the lateral expansion of the products towards the jet. The full explanation of this phenomenon requires, however, numerical simulation of the flow of the two-phase gas-solid particle mixture.

The influence of the W particle content on the efficiency of the jet dispersion is shown in Figures 3(d) and 5. The reactive armour thickness was 10 mm, and α = 30°. Formulations PR-2, PR-3, PR-4 and PR-5 contained 60, 50, 40 and 30% W particles, respectively. All reactive armours were effective for the applied angle of impact. However, it can be seen that reducing the W content results in a slightly lower jet dispersion.

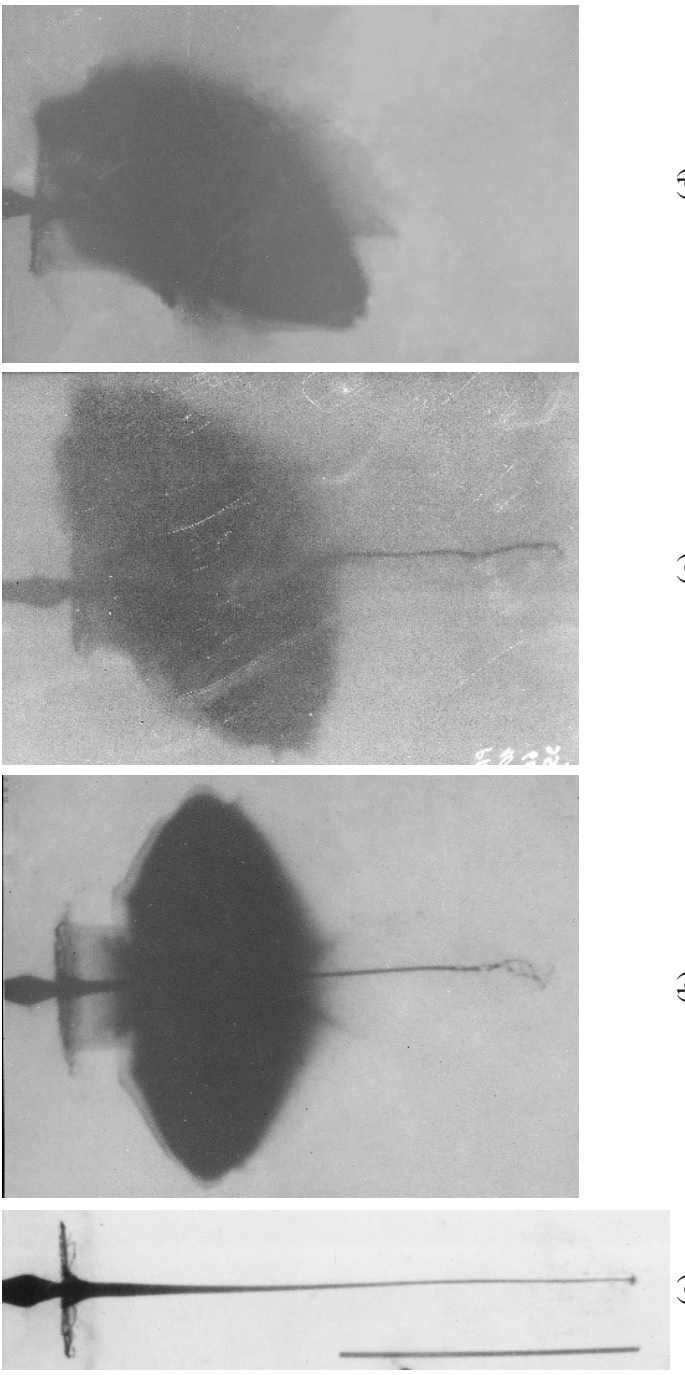

(a) (b) (c) (d)

Figure 3. X-ray photos (inversion) of cumulative jets: no reactive armour (a) and PR-2 reactive armour with thickness of 10 mm and $\alpha = 90°$ (b), 60° (c) and 30° (d)

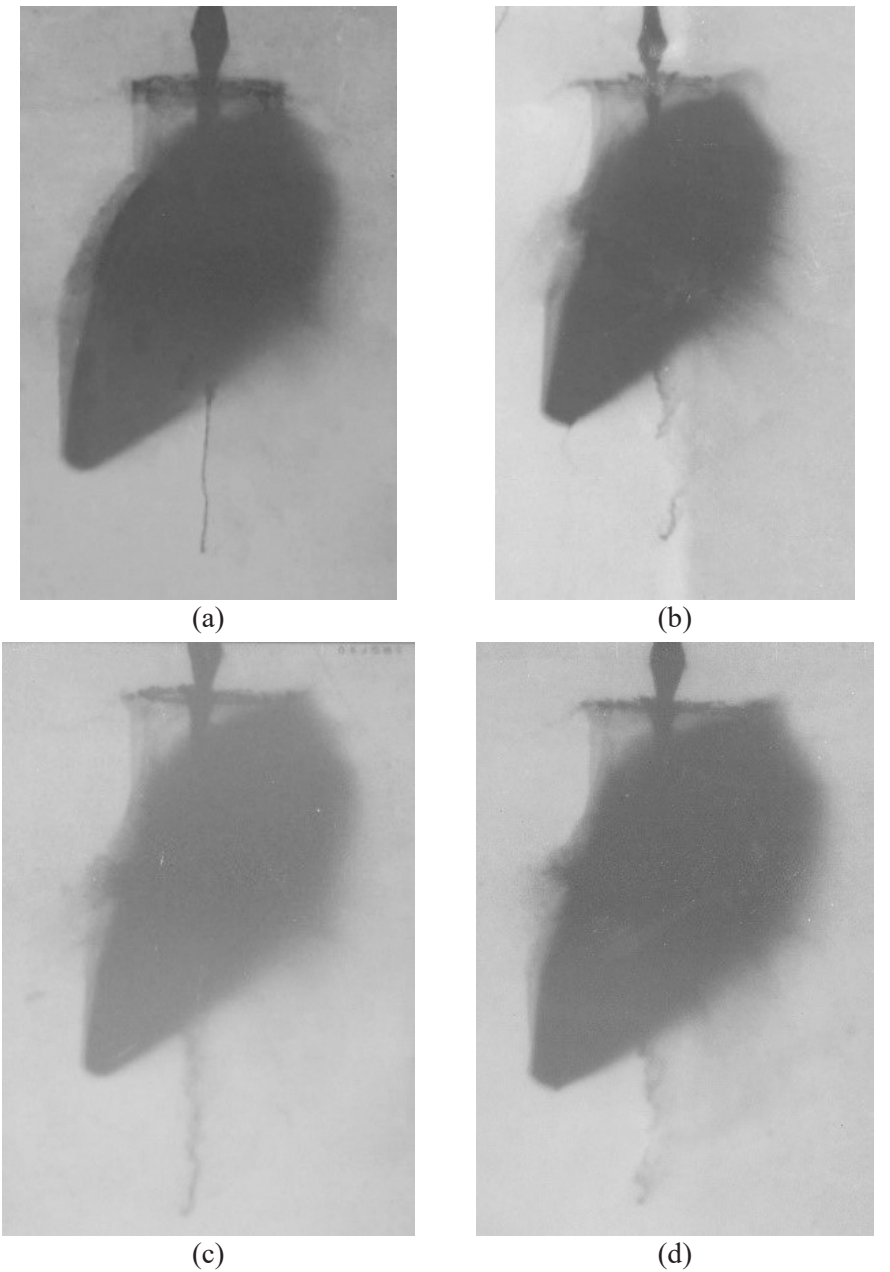

Figure 4. X-ray photos of cumulative jets for $\alpha = 30°$: PR-1, thickness 5 mm (a), PR-1, thickness 10 mm (b), PR-2, thickness 5 mm (c) and PR-2, thickness 7.5 mm (d)

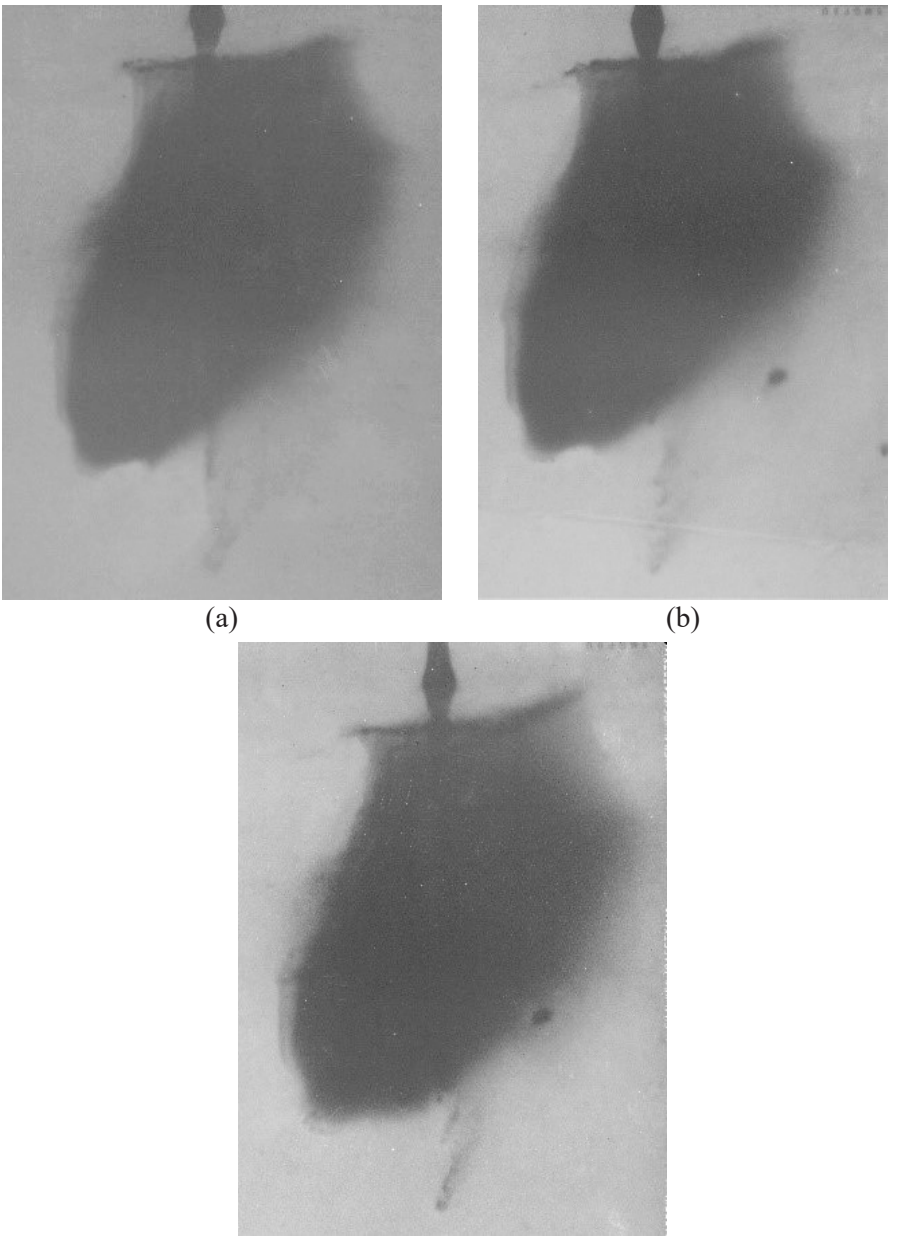

(a) (b)

(c)

Figure 5. X-ray photos of cumulative jets for thickness 10 mm and $\alpha = 30°$: PR-3 (a), PR-4 (b) and PR-5 (c)

Figures 6-8 show fragments of steel witness plates with dimensions of 250×250 mm cut around the holes formed after the impact of the jet particles. The photos in Figures 6-8 correspond to the photos of the jets in Figures 3-5. On the basis of the plate photos, the following parameters were determined: number of holes, total area of holes, diameter of the smallest circle containing all the holes. The values of these parameters are presented in Table 2. Whenever possible, the holes from the slugs were not taken into account. For this reason, the designated area could be overestimated; if the slug hit the place of penetration of the jet particles, its hole could not be separated (Figures 6(c) and 7(b)).

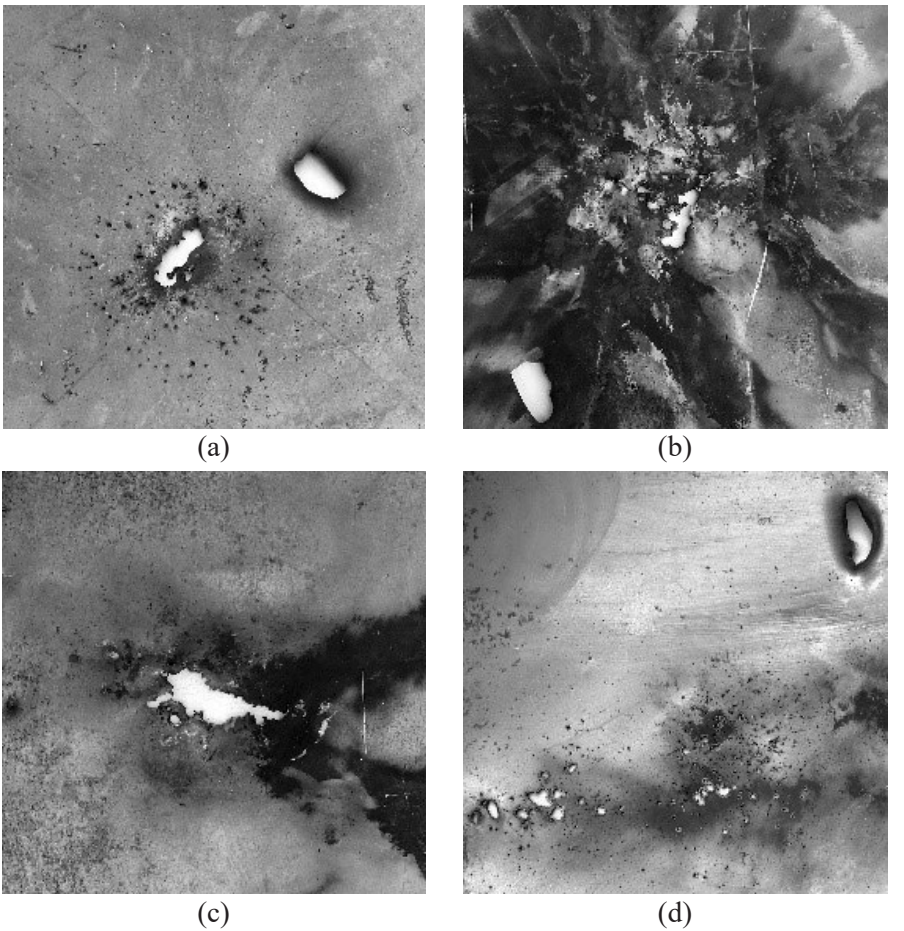

Figure 6. Jet penetration of a steel plate (thickness 10 mm) for no reactive armour (a) and for PR-2, $\alpha = 90°$ (b), 60° (c) and 30° (d)

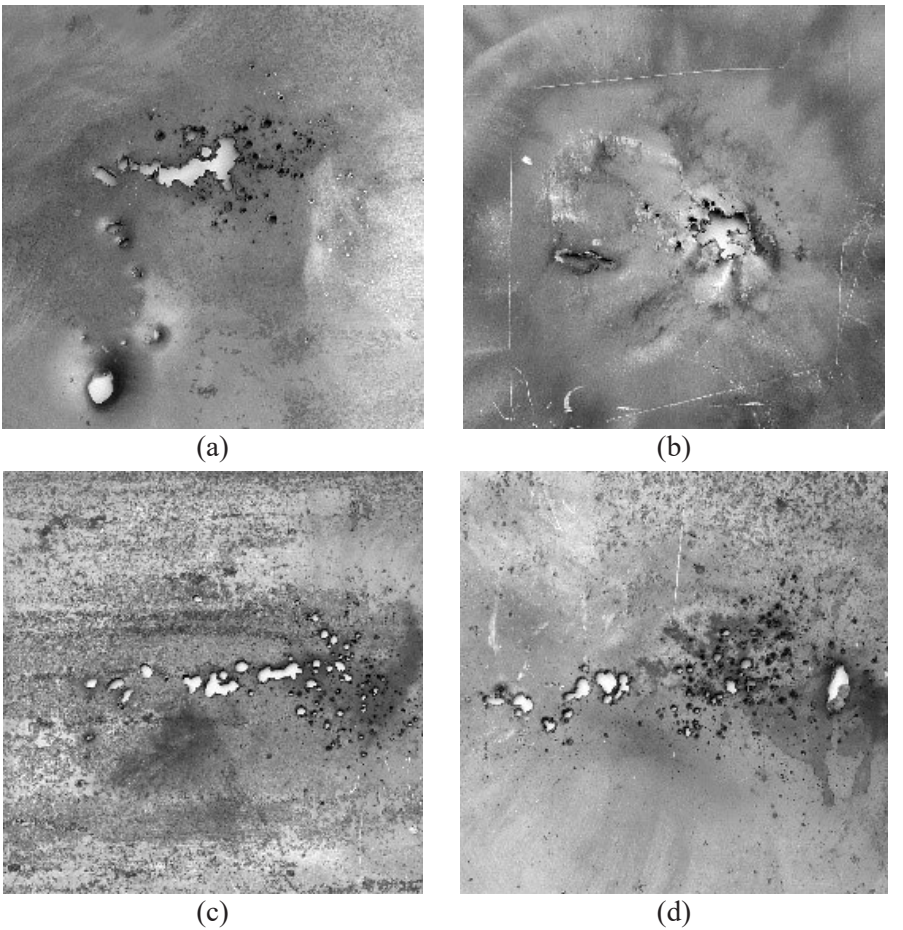

Figure 7. Jet penetration of a steel plate for $\alpha = 30°$: PR-1, thickness 5 mm (a), PR-1, thickness 10 mm (b), PR-2, thickness 5 mm (c) and PR-2, thickness 7.5 mm (d)

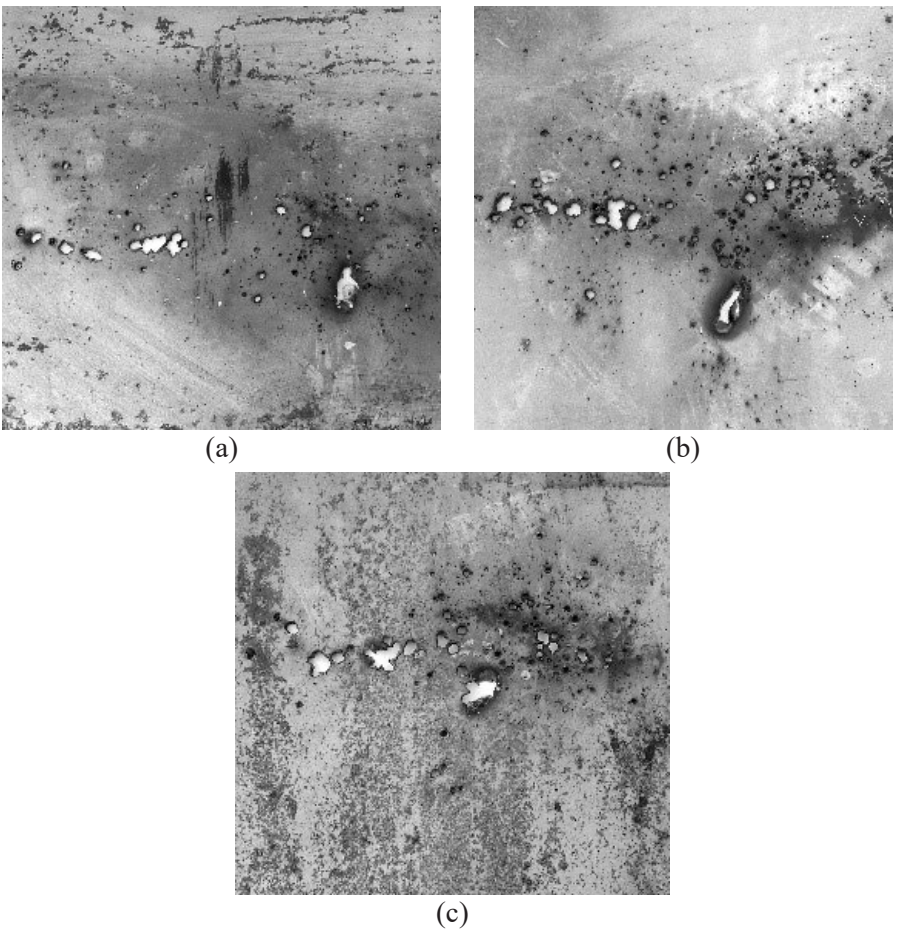

Figure 8. Jet penetration of a steel plate for thickness 10 mm and α = 30°: PR-3 (a), PR-4 (b) and PR-5 (c)

Earlier studies have shown that in the system without the reactive armour, the jet length before fragmentation is 280 mm. Thus, at a distance of approximately 500 mm from the shaped charge the jet was fragmented. At the time of fragmentation, the jet particles may have a small horizontal velocity component, as a result of which they hit the steel plate at different places, punching a large-area hole in it (Figure 6(a), Table 2). The use of reactive armour creates more holes in the plate. In general, an increase in the efficiency of the armour in disturbing the jet should result in an increase in the radius of the circle containing all the holes in the steel plate, an increase in the number

of holes and an increase in the area of the holes. However, the effective disturbance of the jet also produces small particles at a lower velocity which cannot penetrate the 2 mm thick plate. Craters formed after the incidence of such particles were not included in Table 2. Hence, for example, the use of the armour perpendicular to the jet increases the number of holes, but also reduces the total area of the holes (Figure 6(b), Table 2).

Table 2. Number of holes, total area of holes and holes scatter diameter determined from Figures 6-8

Formulation	Layer thickness [mm]	α [°]	Number of holes	Total area of holes [mm^2]	Holes scatter diameter [mm]	Figures
PR-2	–	90	2	429	38	6(a), 3(a)
	10		9	370	55	6(b), 3(b)
		60	7	1055	106	6(c), 3(c)
		30	39	437	177	6(d), 3(c)
	7.5		42	652	178	7(d), 4(d)
	5		50	925	195	7(c), 4(c)
PR-1	10		30	525	176	7(b), 4(b)
	5		33	1111	124	7(a), 4(a)
PR-3	10		39	461	214	8(a), 5(a)
PR-4			43	671	222	8(b), 5(b)
PR-5			43	810	189	8(c), 5(c)

The results from the examination of the angle α on the plate penetration parameters were ambiguous due to the slug hitting the area of impact of the jet particles in the case of $\alpha = 60°$ (Figure 6(c)). The reduction of the reactive armour thickness from 10 to 5 mm for $\alpha = 30°$ caused a slight increase in the diameter of the circle surrounding the holes, but a visible increase in the number of holes and in the total area (Table 2). This means that a greater part of the jet pass through reactive armour of a smaller thickness (Figures 4(c), 4(d) and 3(d)), and that the jet particles have a greater velocity and are able to pierce the plate.

The steel plate data for reactive armour with different W powder contents (PR-2, PR-3, PR-4, PR-5) are presented in Table 2. For W powder contents from 60% (PR-2) to 30% (PR-5), the cumulative jet is effectively dispersed for the angle $\alpha = 30°$ (Figures 6(d) and 8). However, reducing the amount of W causes a significant increase in the total area with a slight increase in the number of holes. The reason for this is the passage of a greater mass of jet through the reactive armour for a lower content of W powder (Figures 3(d) and 5).

A more reliable assessment of the effectiveness of the reactive armour in dissipating the cumulative jet is the depth of the crater in the steel target. Figures 9 and 10 show pictures of the cut targets for selected reactive armour configurations, and Table 3 shows the penetration depth.

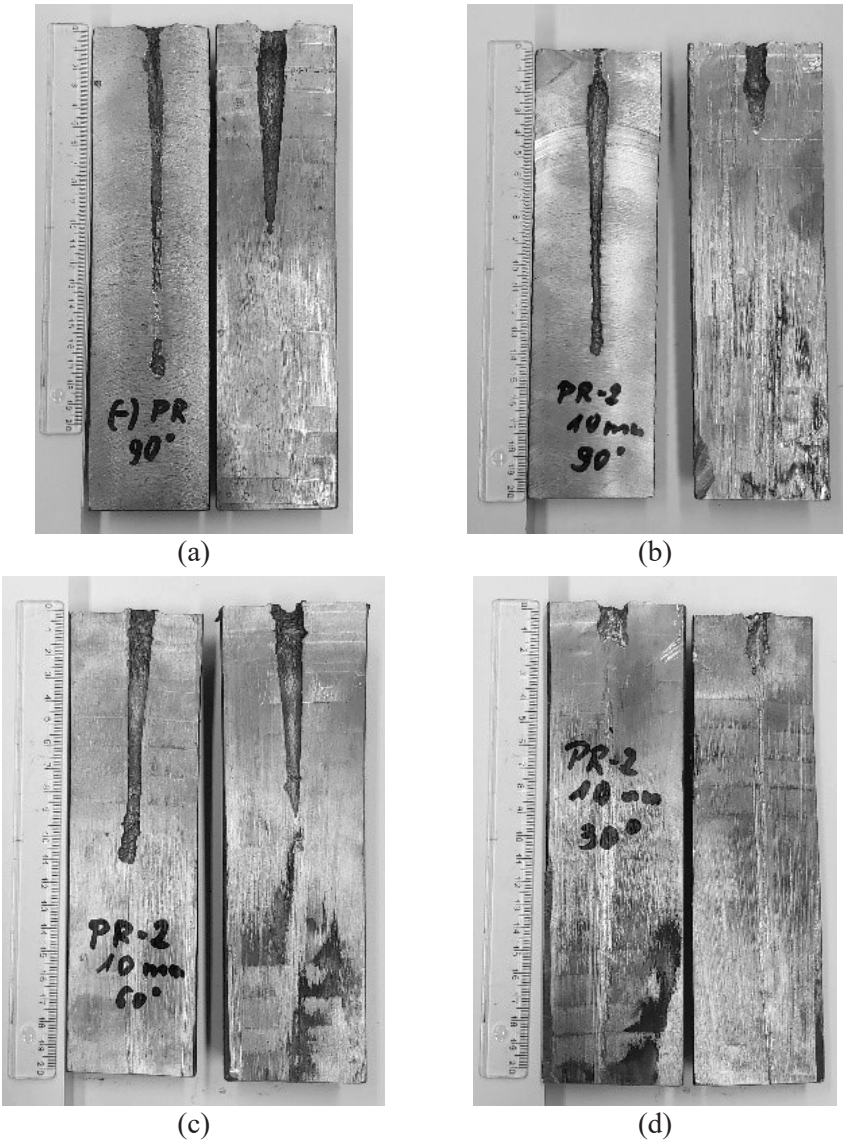

(a) (b) (c) (d)

Figure 9. Jet penetration of a steel target (thickness 10 mm) for no reactive armour (a) and for PR-2, α equals: 90° (b), 60° (c) and 30° (d)

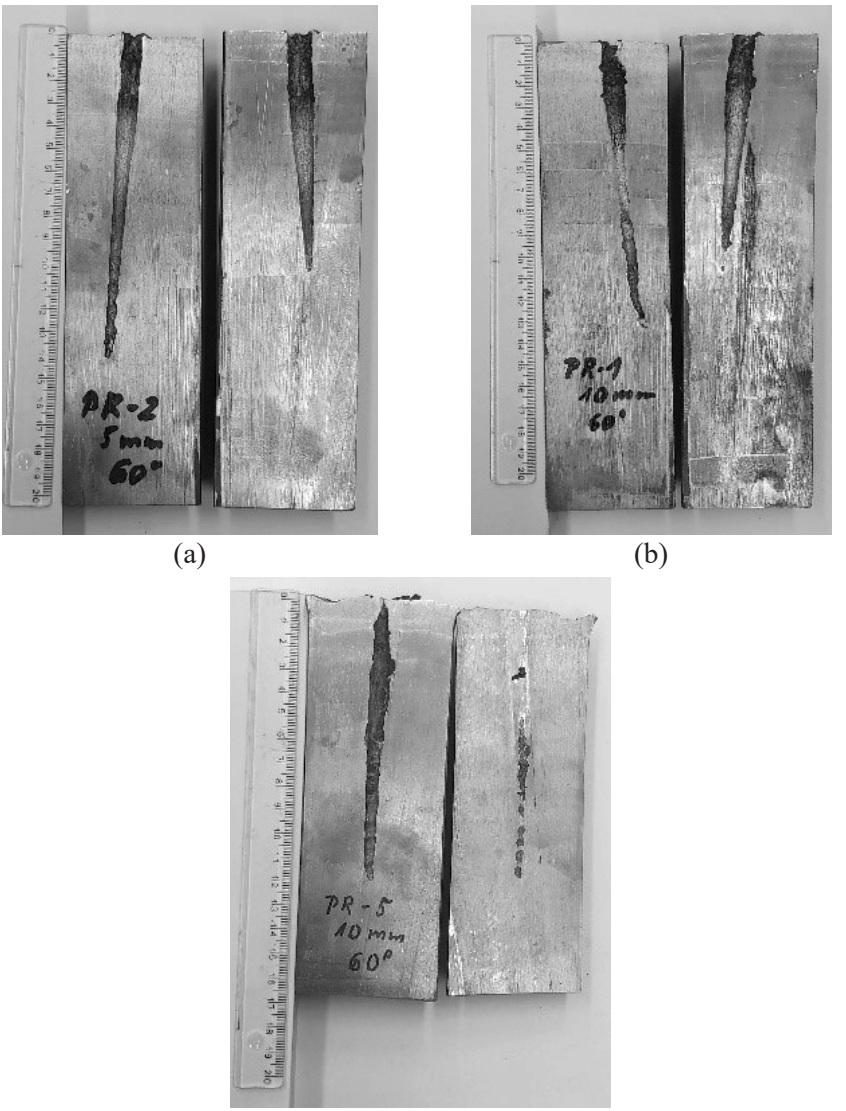

Figure 10. Jet penetration of a steel target for $\alpha = 60°$: PR-2, thickness 5 mm (a), PR-1, thickness 10 mm (b) and PR-5, thickness 10 mm (c)

Table 3. Jet penetration depth in a steel target for tested reactive armour

Armour formulation	Armour thickness [mm]	α [°]	Penetration [mm]	Figures
No armour	–	90	178	9(a), 3(a), 6(a)
PR-2	10		142	9(b), 3(b), 6(b)
		60	112	9(c), 3(c), 6(c)
		30	26	9(d), 3(d), 6(d)
	5	60	140	–
PR-1	10		134	–
PR-5			122	–

The use of any type of reactive armour reduces the crater depth. Decreasing the angle between the direction of the jet and the reactive armour surface causes a reduction in the penetration depth, drastically for $\alpha = 30°$ (Figure 9, Table 3). The craters shown in Figure 9 correlate well with the quality of the jets shown in the photos in Figure 3.

The influence of reactive armour thickness and W powder content on the penetration depth was investigated for $\alpha = 60°$, as for this angle significant differences in the penetration depth were expected. As the reactive armour thickness was increased, the penetration depth of the steel target was decreased (Figures 10(a) and 9(c) for PR-2). The PR-2 armour containing finer W powder protects the steel target better than the PR-1 armour with coarser powder (Figures 9(c) and 10(b)). The penetration depth determined for the PR-5 armour containing 30% W powder was only slightly greater than the penetration depth measured for the PR-2 armour (60% W) of the same thickness (Table 3 and Figures 10(c) and 9(c)).

In order to compare the effectiveness of the explosive reactive armour made from an explosive containing metal powder with classic ERA, armours of such types with the same surface density of ~4.0 g/cm^3 were constructed. The reactive armour of the PR-2 composition was 12 mm thick and was covered on both sides with PLA filament plates 1.5 mm thick and having a density of 1.0 g/cm^3. In the metal ERA, a layer of putty-like explosive [12] with a thickness of 6.5 mm and a density of 1.4 g/cm^3 was placed between two steel plates with a thickness of 2 mm. X-ray pictures of the cumulative jet dispersed by the tested armours set at the angles of $\alpha = 30°$ and 60° are shown in Figure 11, and the results of the penetration of the steel target by the jets in Figure 12 and in Table 4. The traces of the jet on the steel plates (witness) were not analyzed, because large holes appeared after being hit by the ERA plates, which made it impossible to compare them with the plates from the tests with the PR-2 armour.

The analysis of the jet photos taken at the same time (35 μs) from the initiation of the detonation of the shaped charge shows that the jets were more dispersed by the ERA armour. The jets disturbed by the PR-2 reactive armour are thicker. The effectiveness of both types of armour in dispersing the jet was confirmed by the results of the penetration of the steel rod. It should be noted, however, that the PR-2 armour is effective in dissipating the jet for the case of an impact angle of 30°. This fact, combined with the absence of a threat from high-speed driven steel plates, makes it possible to expect that this type of reactive armour will also be used for ballistic protection of vehicles.

(a)

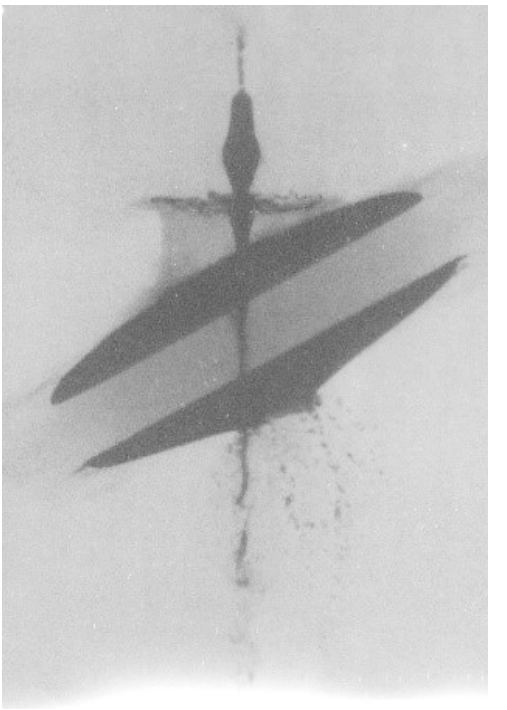

(b)

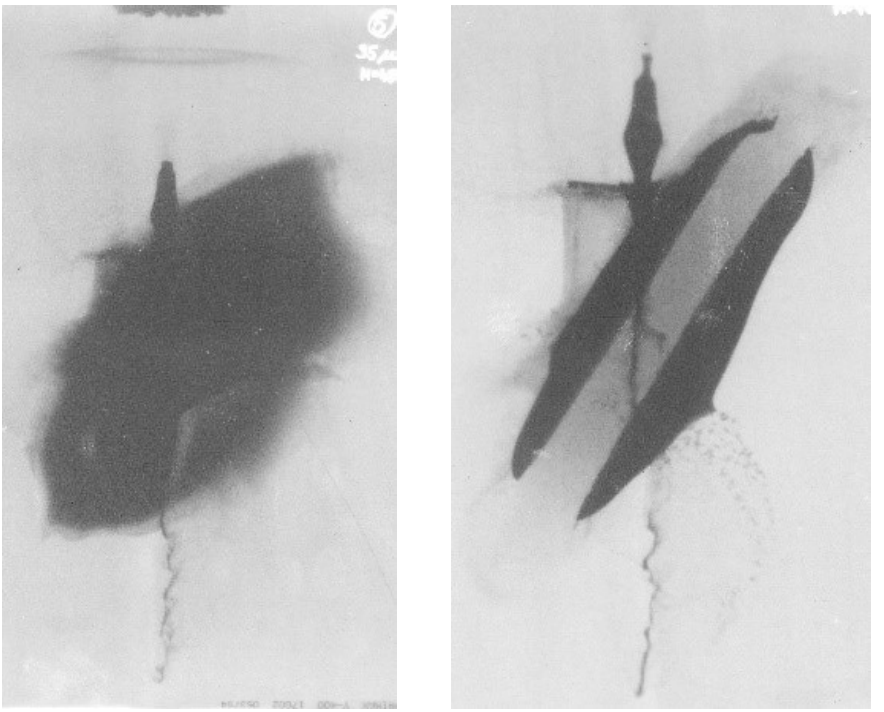

(c) (d)

Figure 11. X-ray photos of cumulative jets: PR-2, $\alpha = 60°$ (a), ERA, $\alpha = 60°$ (b), PR-2, $\alpha = 30°$ (c) and ERA, $\alpha = 30°$ (d)

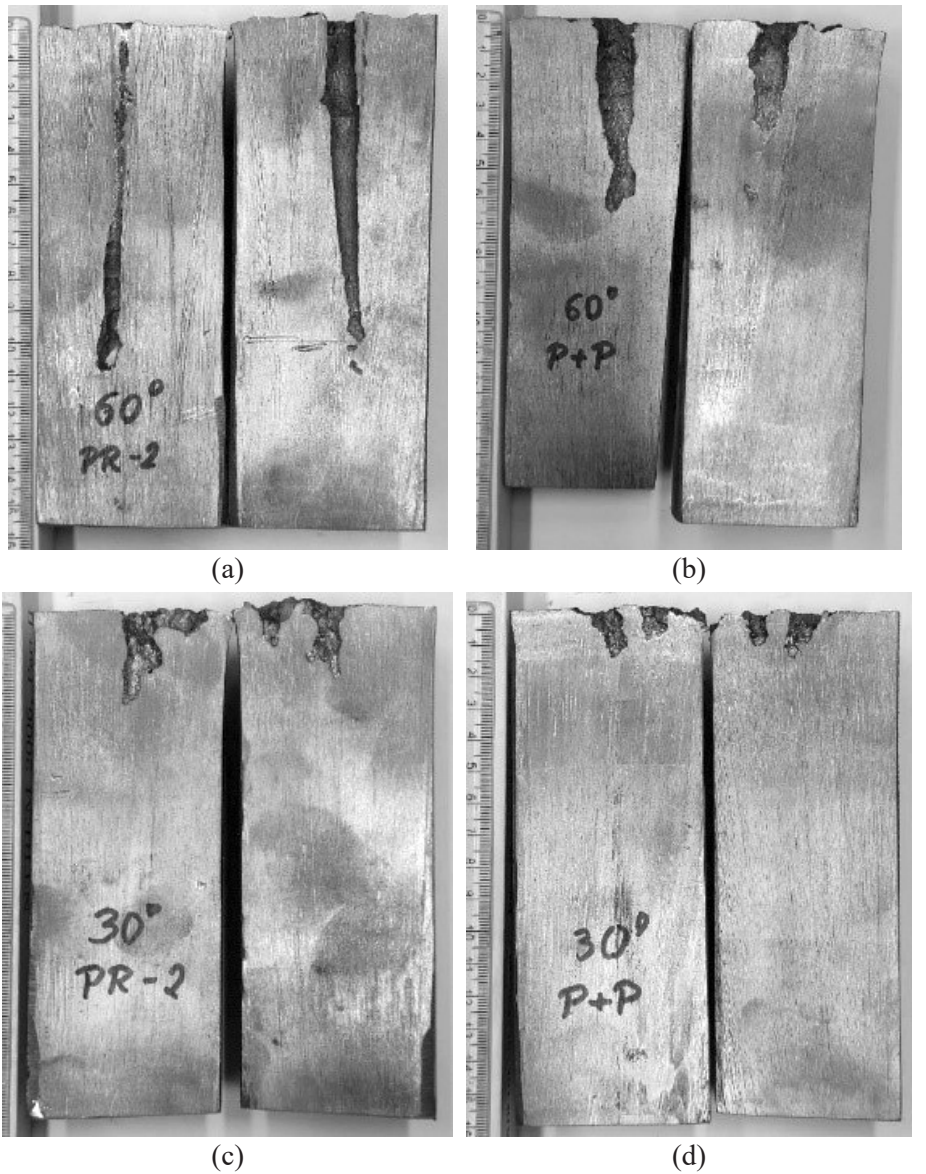

(a) (b)

(c) (d)

Figure 12. Jet penetration of a steel target: PR-2, $\alpha = 60°$ (a), ERA, $\alpha = 60°$ (b), PR-2, $\alpha = 30°$ (c) and ERA, $\alpha = 30°$ (d)

Table 4. Jet penetration depth in a steel rod for the compared reactive armours

Armour type	α [°]	Penetration depth [mm]	Figures
PR-2	60	109	11(a), 12(a)
ERA		66	11(b), 12(b)
PR-2	30	29	11(c), 12(c)
ERA		16	11(d), 12(d)

5. Conclusions

- Reactive armour consisting of HMX, W powder and silicone can effectively disperse the cumulative jet generated by a medium caliber shaped charge. The effectiveness of jet weakening increased with a decrease in the angle between the jet direction and the reactive armour surface. This conclusion was confirmed by the results of examining the penetration depth of the steel barrier by jets hitting the reactive armour at various angles. However, it should be emphasized that a significant reduction in the penetration depth was obtained only for the 30° angle of impact.
- The reactive armour from the formulation containing W particles with an average diameter of 4.5 μm was more effective in disturbing the jet than that containing larger W particles (~35 μm). This was confirmed by the results of the penetration depth test.
- As expected, thicker reactive armour disrupts the jet more strongly, resulting in a significant reduction in the penetration depth of the jet in the steel target.
- A reduction in the W particle content resulted in a slightly lower jet dispersion and, consequently, a slightly greater penetration depth.
- Reactive armour made from an explosive containing heavy metal powder was less effective than the classic ERA. However, taking into account the effectiveness of such reactive armour and the lack of shrapnel threat, this type of reactive armour may be an alternative solution to reactive armour with metal plates.
- The results of the experimental research presented in this paper can be the basis for the verification of mathematical models describing jet dispersion by reactive armour consisting of an explosive and heavy metal particles. They can also be useful in planning further research on the effectiveness of this type of reactive armour in dispersing the jets generated by larger shaped charges.

Acknowledgments

This work was financed by the Ministry of Science and Higher Education through the Military University of Technology under the project UGB 2020-2021.

References

[1] Yael, C.; Sokol-Barak, E.; Friling, S.; Tzalik, M. *Non-Explosive Energetic Material and Reactive Armor Element using Same.* Patent US 7360479, **2008**.
[2] Trzciński, W.A.; Trębiński, R.; Cudziło, S. Study of the Reaction of Model Reactive Armor to Jets Attack. *Propellants Explos. Pyrotech*. **2003**, *28*: 89-93.
[3] Bianchi, S.; Kaufmann, H.; Koch, A. Effect of Ceramics, Fiber Reinforced Plastics and Aluminium used as Confinement Plates for Explosive Reactive Armour. *24th Int. Symp. Ballistics*, New Orleans, USA, **2008**, 520-526.
[4] Mayseless, M.; Bianchi, S.; Kaufmann, H.; Katzir, Z.; Chanukaev, S. Non-metallic Reactive Armor. 27th *Int. Symp. Ballistics*, Freiburg, Germany, **2013**, 1745-1755.
[5] Bhav Singh, B.; Sukumar, G.; Ponguru Senthil, P.; Jena, P.K.; Reddy, P.R.S.; Silva Kumar, K.; Madhu, V.; Reddy, G.M. Future Armour Materials and Technologies for Combat Platforms. *Def. Sci. J.* **2017**, *67*: 412-419.
[6] Cudziło, S.; Dyjak, S.; Trzciński, W.A. Preparation and Characterization of Monolithic Nitrocellulose-Cellulose Composites. *Cent. Eur. J. Energ. Mater.* **2012**, *9*(2): 139-146.
[7] Trzciński, W.A.; Cudziło, S.; Dyjak, S.; Szymańczyk, L. Experimental and Theoretical Investigation of a Model Reactive Armour with Nitrocellulose and Cellulose Composites. *Cent. Eur. J. Energ. Mater*. **2013**, *10*(2): 191-207.
[8] Glikin, L.; Silberman, I.; Friling, S.; Benyami, M. *Reactive Armour.* Patent WO 2018/122844 AI, **2018**.
[9] Mayseless, M.; Asaf, Z. Jet Interaction with High Explosive Flow. *28th Int. Symp. Ballistics*, Atlanta, USA, **2014**, 1064-1075.
[10] *Explosives for Civil Uses – High Explosives – Part 3: Determination of Sensitivity to Friction of Explosives.* (in Polish) Polish Standard PN-EN 13631-3, **2004**.
[11] *Explosives for Civil Uses – High Explosives – Part 4: Determination of Sensitivity to Impact of Explosives.* (in Polish) Polish Standard PN-EN 13631-4, **2004**.
[12] Zalewski, K.; Chyłek; Z.; Trzciński, W.A. Studies on Properties of a Putty-like Explosive with a Silicone Binder. *Cent. Eur. J. Energ. Mater*. **2021**, *18*(1): 112-123.

Received: November 29, 2021
Revised: June 09, 2022
First published online: June 24, 2022